Proceedings of the 18th International Conference on Nuclear Engineering
ICONE18
May 17-21, 2010, Xi'an, China

ICONE18-30217

SODIUM-WATER REACTION ELUCIDATION WITH COUNTER-FLOW DIFFUSION FLAME EXPERIMENT AND ITS NUMERICAL SIMULATION

Akira YAMAGUCHI
Graduate School of Engineering, Osaka University
Suita, Osaka, Japan

Takashi TAKATA
Graduate School of Engineering, Osaka University
Suita, Osaka, Japan

Hiroyuki OHSHIMA
Japan Atomic Energy Agency
O-arai, Ibaraki, Japan

Joji SOGABE
Graduate School of Engineering, Osaka University
Suita, Osaka, Japan

Yoshihiro DEGUCHI
Mitsubishi Heavy Industry
Nagasaki, Nagasaki, Japan

Shin KIKUCHI
Japan Atomic Energy Agency
O-arai, Ibaraki, Japan

ABSTRACT

Sodium-water reaction (SWR) is a design basis accident of a Sodium Fast Reactor (SFR). A breach of the heat transfer tube in a steam generator (SG) results in contact of liquid sodium with water. Typical phenomenon is that the pressurized water blows off, vaporizes and mixes with the liquid sodium. The consequence of the accident are: thermal-hydraulic and chemical impact on the heat transport equipment and structure induced by the heat of exothermic reaction and caustic reaction product.

The purpose of the present paper is to delineate the mechanism and process of the SWR by a counter-flow diffusion flame experiment and a numerical simulation. Based on the numerical simulation, the most appropriate and optimum condition in which stable and continuous diffusion flame of sodium and water vapor is obtained. Key idea is to perform the experiment in a depressurized reaction vessel. According to the experiment, spatial distributions of chemical reactants and products, temperature and particles are measured in detail. The characteristics of the SWR are explained from the present study and the chemical reaction model currently used in the analytical tool of the SWR is appropriate.

1. INTRODUCTION

In a sodium-cooled fast reactor (SFR), liquid sodium is used as heat transfer fluid to carry the energy from the reactor core to the shell and tube type steam generation (SG) system for power generation. The liquid sodium has an excellent heat transport capability and a large safety margin to the boiling point (1153K) at an atmospheric pressure. On the other hand, it has chemical reactivity in contact with water vapor. In the water vapor tube side, the pressure is 17MPa and is 0.2MPa in the sodium shell side, respectively. One of the design basis accidents of the SFR is the water leakage into liquid sodium through a heat transfer tube of SGs, i.e., sodium-water reaction (SWR).

A breach of the heat transfer tube in the SG results in contact of liquid sodium with water. Typical phenomenon is that the pressurized water blows off, vaporizes and mixes with the liquid sodium. The consequence of the accident are: thermal-hydraulic and chemical impact on the heat transport equipment and structure induced by the heat of exothermic reaction and caustic reaction product. Therefore, understanding of the coupled phenomena of thermal hydraulics and chemical reactions are essential to delineate the SWR consequence from the safety viewpoint.

Large-scale experiment series of SWR were performed in Japan (Tanabe and Wachi, 1990). However, the SWR phenomena are generally complex and the experimental measurement technology is not well matured. Therefore, a numerical simulation is used to investigate the coupled phenomena and local quantities such as mass concentrations flow velocities, and temperatures.

According to Takata and Yamaguchi et al. (2005), two chemical reaction types are considered, i.e. a surface reaction and a gas-phase reaction. In the initial phase of the SG tube failure accident, the temperature is well below the sodium boiling point and little sodium vapor exists. Therefore, the water vapor and liquid sodium react at the gas-liquid interface. It is the surface reaction that occurs at the liquid sodium surface. Subsequently, the liquid sodium is heated up by the exothermic reaction. At this stage, sodium vaporizes and the sodium vapor and the water vapor encounter. It results in the gas-phase reaction. In general, most of the sodium remains in the liquid phase because of a large amount of the liquid sodium inventory.

The purpose of the present paper is to delineate the mechanism and process of the SWR by a counter-flow diffusion flame experiment and a numerical simulation. In the gas-phase reaction, one can calculate spatial distributions of the reactants and product including airborne particulates as well as temperature by solving conservation equations. Thus it is advantageous to study the gas-phase reaction under depressurized conditions to understand the characteristics of the SWR. Based on the numerical simulation, the most appropriate and optimum condition in which stable and continuous diffusion flame of sodium and water vapor is obtained. Key idea is to perform the experiment in a depressurized reaction vessel. The numerical simulation tool has been developed foe sodium fire analysis by Yamaguchi and Tajima (2003, 2009). It is modified and extended to the SWR (Yamaguchi and Takata et al., 2006). According to the experiment, spatial distributions of chemical reactants and products, temperature and particles are measured in detail. The validity of the chemical reaction model is investigated based on the discussion of the experimental results.

2. DESIGN OF DIFFUSION FLAME EXPERIMENT

A sketch of the SWR is shown in Fig. 1. A breach of a heat transfer tube in the SG results in sudden influx of the water and steam into liquid sodium. The water turns to the vapor phase by sudden depressurization in quite a short time. Typical phenomenon is that the pressurized water and steam blows off and mixes with the liquid sodium where many heat transfer tubes exist. At the interface of the liquid sodium and the water vapor, the SWR takes place and reaction heat and reaction products, i.e. sodium hydroxide and hydrogen mostly are generated as follows:

$$Na_{(\ell)} + H_2O_{(g)} \rightarrow NaOH_{(\ell)} + \frac{1}{2}H_2 \quad (1)$$

$$2Na_{(\ell)} + H_2O_{(g)} \rightarrow Na_2O_{(\ell)} + H_2 \quad (2)$$

The temperatures in the sodium side are 625K and 743K for cold leg and hot leg, respectively. The sodium is in liquid phase because the boiling temperature is greater than the system temperature by 500 K.

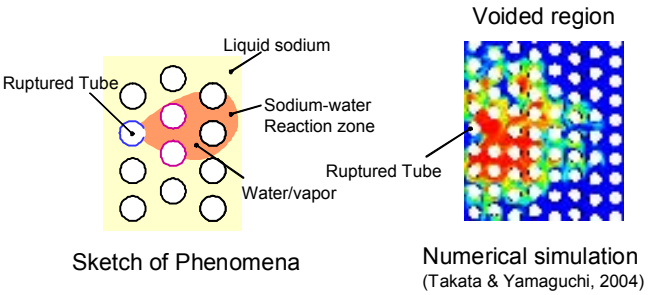

Fig. 1 Sketch of the sodium water reaction phases.

For delineating the SWR phenomena at the liquid-solid interface, a test vessel for counter-flow diffusion flame experiment has been developed (Yamaguchi and Takata, 2009). Figure 2 shows the test vessel and gas flow conditions and measurement points schematically.

The outline of the experiment is as follows. A liquid sodium pool is heated up to 800K (less than the boiling point by 253K) so that the sodium evaporates slowly. The sodium pool diameter is 30 mm and the liquid sodium mass in the pool is 1.7 grams. Through the nozzle above the liquid pool surface, water vapor diluted to 2.0 volumetric % by argon gas flows out toward the sodium pool surface. Hence a counter flow diffusion flame is formed between the pool surface and the flow nozzle. It is important to keep the water vapor density at very low value for visualizing the flame zone. Otherwise, we cannot see the experimental cell inside because it is filled with white smoke (reaction product aerosol of sodium hydroxide). A strainer is installed at the exit of the mixture gas flow to provide flat velocity distribution. The reaction zone exists in-between the sodium pool and the strainer.

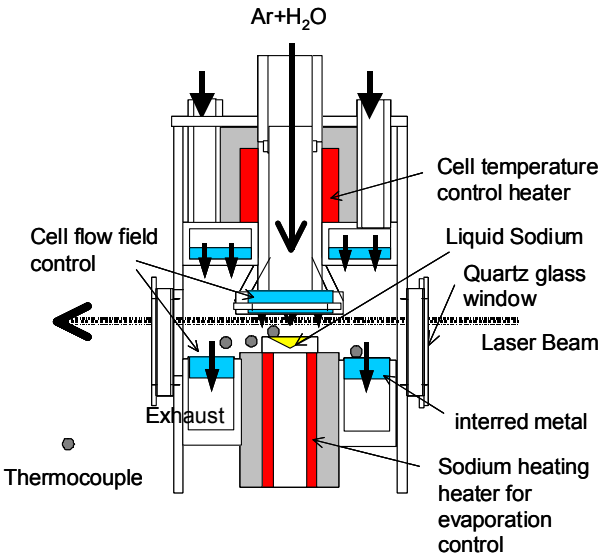

Fig.2 Sodium-water counter flow diffusion flame experiment

The test conditions and geometries of the pool and the test vessel are determined based on the numerical simulation. Requirement on the experiment are (1) the diffusion flame of the sodium and water is stable and completely reproducible; (2) the diffusion flame is sustainable foe ten minutes or more for the measurement of the temperature and concentration field; (3) the reaction zone is broad enough from the viewpoint of spatial disolution; (4) the chemical reaction products in particle (i.e., sodium hydroxide, sodium oxide, etc) do not deteriorate the transparency and visibility for the laser measurement; (5) the reaction zone is axisymmetric and, in addition, one dimensional around the pool center.

Try and error type simulations are performed so that the above mentioned requirements are achieved. The sodium pool is heated up to 820K which is equivalent to or higher than the SFR coolant condition. Sufficient sodium vapor flux is obtained at the temperature level. The water vapor is diluted by inert Ar gas to 2.0 volumetric percent. It is heated, uniformed and flows downward to the sodium pool surface. Surrounding the Ar and H2O flow, downward Ar flow (inner guard flow)is given which keep the water vapor flow one dimensional and prevent the water vapor does not disperse in radial direction. In addition, another Ar gas flows (outer guard flow) downward in the peripheral of the test vessel. The flow is supposed to remove the particle-like chemical reaction products from the reaction region efficiently. The flow velocity and the temperature of the outer guard flow are decided so that the reaction region is kept visible from the quartz glass window. The sodium pool geometry is conical which will minimize the influence of the sodium level change by the vaporization. Lastly the test vessel is depressurized to 0.042MPa. The reaction region is stretched and move upward that is helpful for the accurate measurement.

According to the numerical simulation, the flow field shown in Fig. 3 is predicted. The water vapor encounters the sodium vapor and reacts. The reaction products are removed by the guard flow which turns to the radial flow. A part of the outer guard flow is stagnant or forms secondary circulation at the pool peripheral. With this guard flow, the water vapor does not attach to the pool surface. In the preliminary experiments, it is observed that the sodium in the pool is consumed in quite a short time if the water vapor collides to the liquid sodium directly. It suggests the characteristics of the surface reaction and gas-phase reaction.

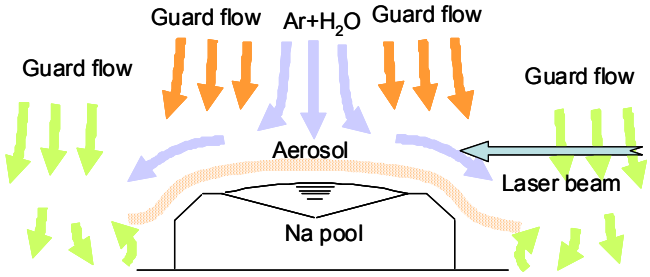

Fig.3 Sodium-water counter flow diffusion flame experiment

Figure 4 shows the numerical prediction of the particle-like reaction products in the present experiment. The analytical condition is shown in the figure. The reaction zone is approximately 8-10 mm above the pool surface where the reaction products appear. It is confirmed that one-dimensional concentration distribution at the pool center is obtained. The reaction products exist below the reaction zone. At the pool peripheral, the particles flow in radial direction and downward as shown in Fig. 3. The particle distribution will not influence the transparency in the laser measurement.

For comparison, Figure 5 shows the composite photograph of the reaction zone before the sodium pool geometry and the test conditions are optimized. The reaction zone as well as the aerosol mass concentration taken in the experiment is shown in this figure. Blue color shows the OH radical fluorescence intensity measured by the Laser-Induced Fluorescence (LIF) technique. It is seen that the reaction zone lied in 2-3 mm above the pool surface. The aerosol concentration is visualized by the scattering of the laser beam from the aerosol particles. We can see the red light emission from the levitating aerosols. The aerosol existing area is like “crown” shape. It is understood that the visibility and reaction zone in Fig. 3 is

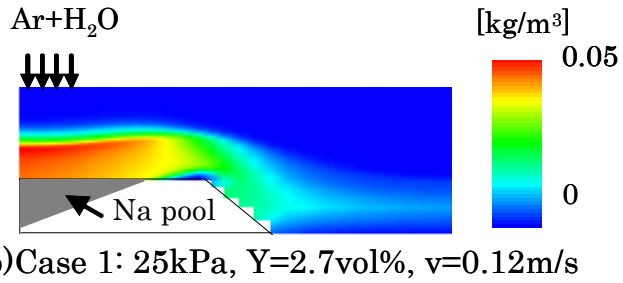

(b)Case 1: 25kPa, Y=2.7vol%, v=0.12m/s

Fig. 4 Particle (aerosol) mass concentration distribution from numerical simulation.

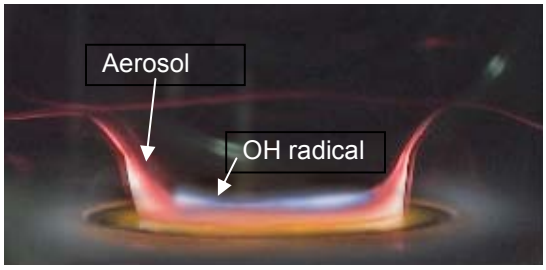

Fig. 5 Visualization of sodium-water reaction (Yamaguchi and Takata, 2006)

3. FINDINGS FROM DIFFUSION FLAME EXPERIMENT

Figure 6 show the photo in the present experiment We can see the self-luminescence and the laser scattering. Comparing Fig. 6 with Fig. 4, it is seen that similar particle concentration and reaction zone geometry are obtained between the experiment and the numerical simulation. The self luminescence appears 10mm above the pool surface. Between the self-luminescence and the pool surface is the laser scattering that comes from the reaction product. These characteristics are axisymmetric. The visibility of the reaction region is quite satisfactory. The photos at 5 minutes and 10 minutes after the beginning of the reaction are compared. No difference is seen between the photos. It is concluded that the stable diffusion flame continues for ten minutes at least, which is enough long for the measurement. To check the influence of Ar gas purity on the self-luminescence, two types of Ar gas are used, i.e., 99.99% and 99.9999% purified, respectively. No influence is observed for the two cases. Several experiments are performed with the same condition and the reproducibility of the diffusion flame is excellent.

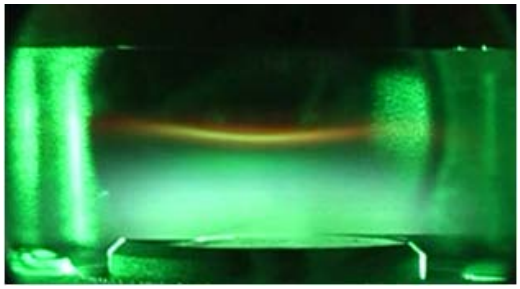

Fig. 6 Visualization of sodium-water reaction

Radial temperature distribution is measured at 19mm above the pool surface which corresponds to the elevation of the Ar and H2O gas flow outlet. Figure 7 shows the temperature profile of thermocouples T4 and T7. The two thermocouples are scanned in perpendicular radial directions each other. It is seen the water vapor flows out of the nozzle at the temperature 700K. Although the temperature gradually decreases to the test vessel temperature in radial direction, uniform distribution is obtained around the measurement lined above the pool. Also the temperature distribution is almost axisymmetric.

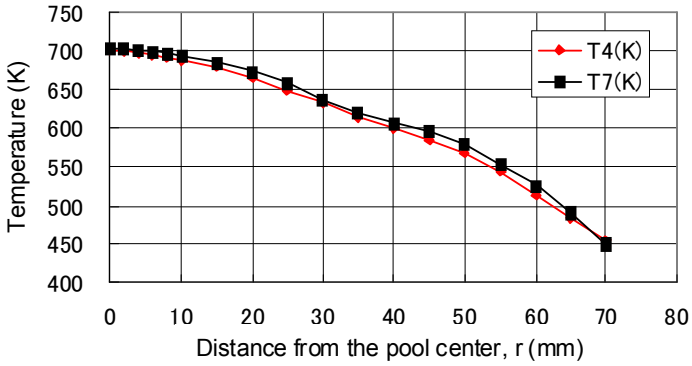

Fig. 7 Radial gas temperature distribution 19mm above the pool surface.

Let us discuss the self-luminescence observed 10 mm above the pool surface. The spectrum of the luminescence is evaluated. The characteristic wave length is 589nm, that is D line of sodium (transition from t3p orbit to 2s orbit). It is interesting that the luminescence appears at 10mm above although the sodium vapor density should be maximum at the pool surface.

To investigate the phenomenon, another experiment is performed in which the water vapor line is closed and only Ar gas is provided to the test vessel. Two photos are taken. The right hand photo in Fig. 8 shows the Mie scattering with the 532nm laser sheet while the photo in the left is the visual frame. It is seen that no self-luminescence is observed if the water

vapor does not exist. Thus it is concluded the luminescence is induced by the activation of sodium caused by the sodium-water contact. On the other hand, the right photo in Fig. 8 indicates the existence of particles that scatter the laser sheet. In the experiment condition in the right photo in Fig. 8, only sodium vapor and Ar exists. According the results, it is concluded that the sodium vapor which is originally 820K at the pool surface contact with the Ar gas flow of 700K resulting in the sodium condensation. Hence the particle-like sodium mist scatters the laser beam and the Mie scattering is observed.

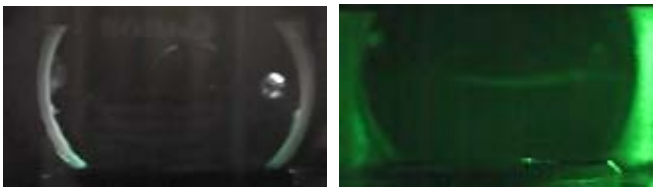

Fig. 8 Photo of visualization with no water vapor (right: with laser sheet, left: no laser sheet).

In the next experiments the photo is taken with the water vapor. Likewise Fig. 8, the right photo is with the laser sheet. The laser is not irradiated in the left photo. Several new facts are found comparing Figs. 8 and 9. First, the self-luminescence is the D line of sodium that is caused by the reaction process of sodium and water because it is observed only if the sodium and water encounters. Secondly, particle like material exists at the reaction region and between the pool and the reaction region. The former is the condensed sodium vapor (sodium mist) and the latter is the reaction products levitating in the sodium vapor.

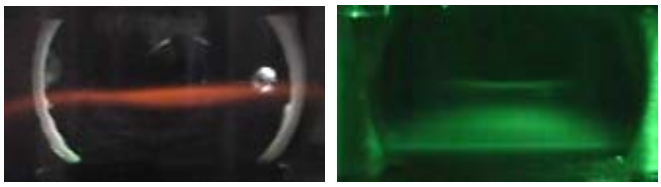

Fig. 9 Photo of visualization with water vapor (right: with laser sheet, left: no laser sheet).

In the experiment, the temperature distribution, the concentrations of hydrogen, water vapor, sodium vapor, OH, particles, and O are measured along with the vertical directions above the pool center. Figure 10 shows all the distributions at a glance.

Fig. 10 Temperature and concentration distributions along with the pool center line.

The temperature distribution is measured to identify the reaction region in comparison with other quantities. Although a notable temperature peak does not to exist in Fig. 6, it seems the temperature at 11-12mm from the pool surface seems to be higher. According to Takata, Yamaguchi et al (2004), overall reaction heat of the separation of H2O to OH and H and the connection of Na and OH is endothermic. Considering the binding energy of hydrogen, the overall reaction is exothermic. The hydrogen of 0.5-1.0% is observed in the reaction region experiment at atmospheric pressure. Therefore, the hydrogen

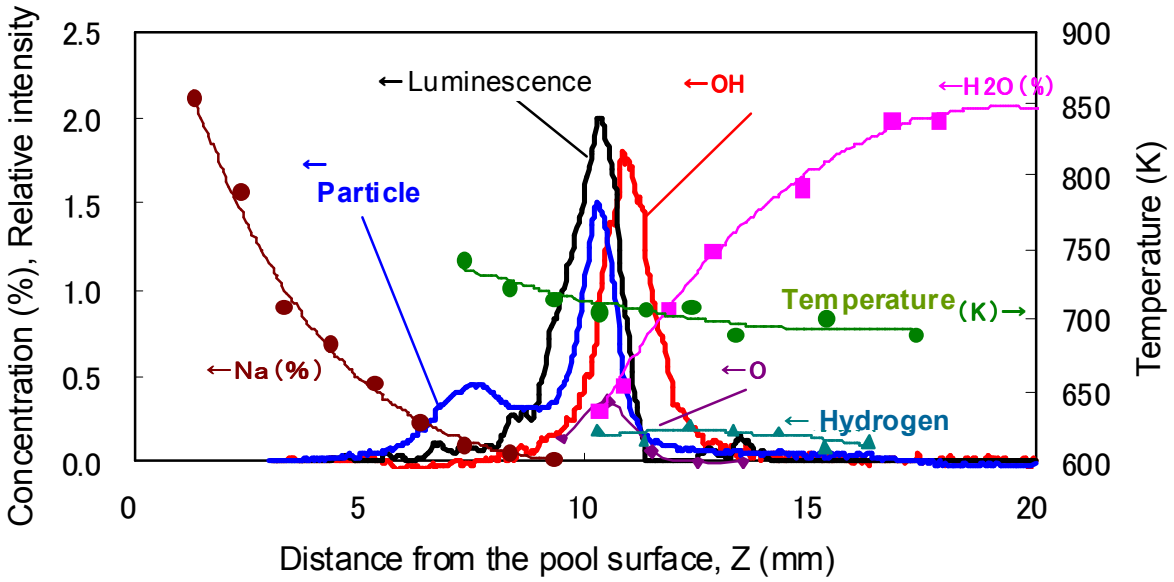

Fig. 10 Temperature and concentration distributions along with the pool center line.

concentration in Fig. 10 may correspond to the reaction region at 11-12 mm. The hydrogen concentration is measured with CARS technique and it could not be measured below 10 mm because of the noise from the sodium. With regard to the temperature and hydrogen distributions, it suggests the location of the reaction region. However, the temperature rise and hydrogen concentration is not clear in Fig. 10. Comparison with the numerical simulation and another experiment specially designed for this purpose are the important work in the future.

Water vapor is supplied at 2.0 volumetric percent of the concentration. The saturated vapor pressure of sodium at 820K is 1.38kPa. Thus the volumetric concentration is 3.3 percent at the test pressure, 42kPa. It can be said that the reaction region exists around 10mm from the pool surface because the reactants, i.e. sodium vapor and the water vapor disappear at this location. The water vapor concentration decreases linearly between 13-10 mm. It implies the water vapor consumption velocity is high and the chemical reaction is controlled by the mass transfer velocity. On the other hand, the sodium vapor is decreasing between 0-3 mm linearly above which the concentration gradient becomes less steep. Figure 11 shows two experimental results of the sodium vapor concentration with the same conditions. Reproducibility is good enough. From 3 mm to 10mm, the sodium vapor flux is decreasing which suggests the sodium is consumed before it reaches to the reaction zone. In other words, the gas-phase reaction rate is relatively small since the sodium is not efficiently contributes to the sodium water reaction. It is considered that the gas-phase reaction takes place in water vapor rich and sodium dilute condition.

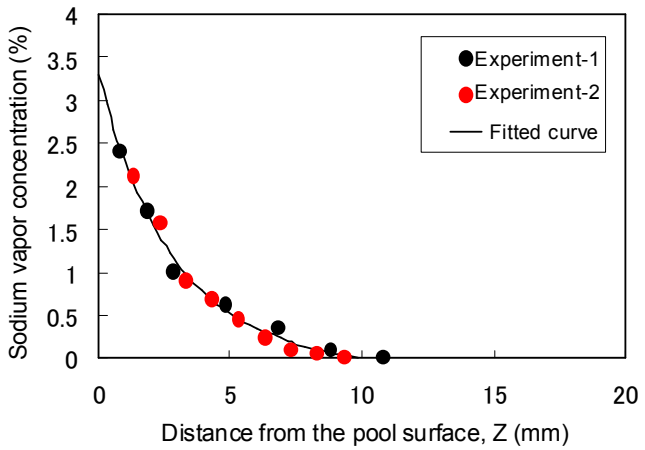

Fig. 11 Sodium vapor concentration in two independent experiments.

OH radical measurement shown in Fig. 10 indicates that OH radical exists above the self-luminescence region. It is considered that the location z=13 mm is the upper end of the reaction region. The water vapor concentration is varied from 1.7% to 2.3%. As the concentration increases, the peak location moves toward the pool surface as expected. It is noted, however, the reaction characteristics and the relative location of the reactants and products are not changed. Also, in every test condition, the counter flow diffusion flame is very stable.

As to the particles measurements, the Mie scattering and the self-luminescence are already discussed in Figs. 8 and 9. In Fig. 10, it is noted that two peaks appear at z=10mm and 7-8 mm. The results correspond to the visual observation in Fig. 9. Two types of measurement are performed here, i.e. Mie scattering and Laser Induced Incandescence (LII). The intensity of Mie scattering is proportional to the 6th power of the particle diameter and LII signal intensity is related to the 3rd power of the diameter. Thus if we compare the two intensities we can obtain the average particle diameter distribution as well as the particle volume fraction distribution. The results are shown in Fig. 12. It is seen that the particle diameter becomes larger at the pool surface. The coagulation process of the particles is the reason of the phenomenon. Another point is the comparison of Fig. 4 (numerical simulation) and Fig. 12. In the numerical simulation, we can see only one maximum at z=6-7 mm. It is because the numerical simulation takes sodium vapor and the reaction products into consideration. As mentioned above, the peak at z=10mm may correspond to the sodium mist which is caused by the sodium vapor condensation. Also the sodium consumption between the sodium pool surface and the reaction region is not considered in the simulation. Comparison of the experimental results and numerical simulation is necessary that take into account the sodium monomer and dimer, interaction of the sodium vapor and particle, and the condensation of sodium vapor.

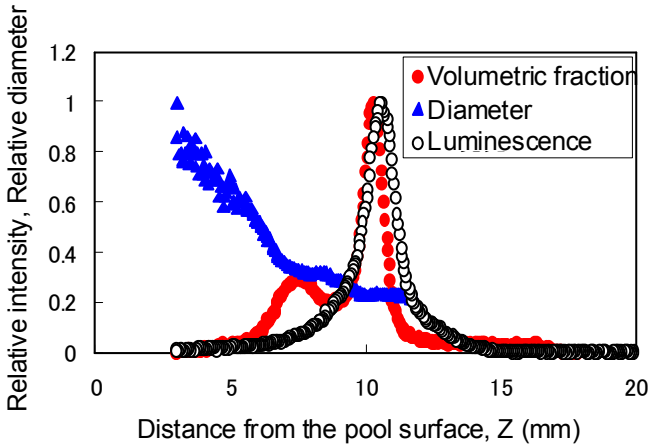

Fig. 12 Particle volumetric fraction and diameter distributions.

Lastly, existence of O atom is measured. It is confirmed that the O atom exists at the similar location of the self-luminescence. Although the measurement of O atom has less accuracy, this result suggests the sodium atom is activated and emits light around 10 mm where the water vapor decompose to OH and O.

The reaction products remained in the pool are analyzed after the experiments. Important results are obtained, i.e. sodium hydroxide is observed at the peripheral zone of the pool bottom. On the other hand, in the center of the pool bottom, both the sodium oxide and sodium hydroxide are observed. The particle-like chemical reaction products sediment on the sodium pool. At the pool peripheral, it is natural to consider the reaction products settle. At the pool center, the reaction products sink in the sodium pool and stayed for the time being in the sodium-rich conditions. In addition, experiments are performed in which the water vapor concentration is increased to 11% and the reaction products remained in the pool bottom is analyzed. In this case, only the sodium hydroxide is measured. From the observations, the conclusions that the authors recognize is that sodium hydroxide is generated during the SWR process. If the reaction product (mostly NaOH) transported to sodium rich environment, sodium oxide (Na2O) is generated.

4. REACTION MECHANIZSM OF SWR

Here, the observations from the experiments and some supporting evidence from the numerical simulation are summarized in the following:

(1) The reaction region lies ranges 9-12mm from the pool surface. In this region, self-luminescence of the sodium and the existence of the OH radical are observed. The OH radical exists above the sodium self-luminescence. In the sodium self-luminescence region, a small amount of O atom is observed.

(2) Above the OH radical existing region, it seems the gas temperature increases slightly. It may correspond to the peak location of the hydrogen. The results suggest the hydrogen molecular is generated in this location. However, it is important that we recognize the temperature rise and the hydrogen concentration peak are not clear. More investigation is necessary on this point.

(3) The reaction rate of the water vapor is rapid. The slope of the water vapor concentration is almost linear. The consumption velocity of the water vapor is controlled by the transport velocity.

(4) It is suggested that the sodium vapor is consumed before it reaches to the reaction region. The sodium reaction rate is relatively slow. The slope of the sodium vapor concentration is linear at the pool surface but becomes less steep above 4mm from the pool surface and almost flat at the reaction region. It is a future work to investigate the mass balance and the status of sodium vapor.

(5) Particles exist in the same region as the self-luminescence. The particle volume fraction distribution exhibit two peaks. One is in the reaction region. The other is in-between the pool surface and the reaction region. It is desirable to clarify the particles constituents. Are the particles, in other words, condensed sodium, reaction products, or mixture of the reaction product and the condensed sodium?

(6) SWR in the gas phase generate NaOH and hydrogen. Na2O is observed deep in the liquid sodium pool.

5. CONCLUSIONS

Sodium-water reaction process is delineated by the counter-flow diffusion flame experiment under the depressurized situations. Major observations are summarized in section 4.

In conclusion, the author would like to emphasize several points. The computer program developed for the SWR is effectively used in the experiment design and the interpretation of the experimental results. The experimental technique and now-how are accumulated to understand the SWR phenomena. An experiment to investigate the SWR is very difficult because of high temperature and pressure, highly corrosive chemical reaction products, invisibility of the reaction region, difficulty in the mass spectrometry. The detail of the SWR process is delineated in the present study. It has not been well understood because of the reason mentioned above.

Future work is the comparison of the experiment and the numerical simulation in detail. Through this process, whole picture of the SWR would be depicted and the knowledge, numerical tool and the experimental database would be effectively used in the development of the SFR.

REFERENCES

H. Tanabe and E. Wachi, “Review on Steam Generator Tube Failure Propagation Study in Japan”, *Proc. of IAEA/IWGFR Specialists’ Meeting on Steam Generator Failure and Failure Propagation*, p. 33-35, Aix-en Provence, France (1990).

T. Takata, A. Yamaguchi, K. Fukuzawa and K. Matsubara, "Numerical Methodology of Sodium-Water Reaction with Multi-Phase Flow Analysis", *Nucl. Sci. and Engineering*, 150, 221-236, 2005

Yamaguchi, A., and Tajima, Y., 2003, Numerical Simulation of Non-premixed Diffusion Flame and Reaction Product Aerosol Behavior in Liquid Metal Pool Combustion, *Journal of Nuclear Science and Technology*, 40(2), 93-103.

Yamaguchi, A., Takata, T., Ohshima, H. and Suda, K., Sodium-Water Reaction and Thermal Hydraulics at Gas-Liquid Interface: Numerical Interpretation of Experimental

Observation, ICONE14-89615, Proceedings of 14th International Conference on Nuclear Engineering, July 17-20, 2006, Miami, Florida, USA

